

## Effect of Organic Corrosion Inhibitors on the Corrosion Performance of 1018 Carbon Steel in 3% NaCl Solution

L.M. Rivera-Grau<sup>1</sup>, M. Casales<sup>2</sup>, I. Regla<sup>2,3</sup>, D.M. Ortega-Toledo<sup>2</sup>, J.A. Ascencio-Gutierrez<sup>2</sup>, J. Porcayo-Calderon<sup>1,\*</sup>, L. Martinez-Gomez<sup>2,4</sup>

<sup>1</sup> Universidad Autonoma del Estado de Morelos, CIICAp, Av. Universidad 1001, 62209-Cuernavaca, Morelos, Mexico

<sup>2</sup> Universidad Nacional Autonoma de Mexico, Instituto de Ciencias Fisicas, Av. Universidad s/n, Cuernavaca, Morelos, Mexico

<sup>3</sup> Universidad Nacional Autonoma de Mexico, Facultad de Estudios Superiores Zaragoza, Mexico D.F., Mexico

<sup>4</sup> Corrosion y Proteccion, Buffon 46, Mexico City, C.P. 11590, Mexico

\*E-mail: [jporcayoc@gmail.com](mailto:jporcayoc@gmail.com)

*Received:* 5 November 2012 / *Accepted:* 7 December 2012 / *Published:* 1 February 2013

---

The corrosion inhibition of 1018 carbon steel in 3% NaCl solution at 50°C with imidazoline-based inhibitors has been evaluated by using electrochemical techniques. Techniques included polarization curves, open circuit potential, linear polarization resistance and electrochemical impedance measurements. The results showed a low performance of the inhibitors. However, it was observed that inhibitors either can be adsorbed on the substrate surface or modify the solution resistivity and thereby enhanced the corrosion performance.

---

**Keywords:** 1018 carbon, NaCl corrosion, inhibitors, electrochemical techniques

### 1. INTRODUCTION

Carbon dioxide (CO<sub>2</sub>) corrosion of pipeline steels and equipment has been considered one of the most severe problems in the oil and gas industry where carbon steels are commonly used for different purposes, because of its cost effective characteristics. However, carbon steel is not the most corrosion resistant for many environments. The low corrosion resistance of carbon steel is due to its inability to develop a protective oxide layer on its surface that protects it from the aggressiveness of the surrounding environment. It has been demonstrated that carbon steel can be safely operated in very

corrosive service conditions if the corrosion control system is properly designed and implemented. In order to reduce the corrosion of carbon steels, inhibitors are frequently added to the produced fluid to control corrosion as an economical and flexible method. Inhibitors can adhere to metal surface to form a protective barrier against corrosive agents contacting with metal. The efficiency of an inhibitor to provide corrosion protection depends to a large extent upon the interactions between the inhibitor and the metal surface [1].

The use of organic corrosion inhibitors is the most effective way of protecting internal corrosion of carbon steel pipelines for oil product transportation. Nitrogen-based organic surfactants, such as imidazolines or their salts have been used successfully as corrosion inhibitors in the oil and gas industries even without an understanding of the inhibition mechanism [1-5]. However some studies have been reported for a better understanding of the mechanisms by which inhibitors protect the surface of the materials. The electron configuration of several imidazoline inhibitors by the quantum chemical calculation has been studied, and it was found that electron donor group introduced, particularly, the substituent group with conjugated system, to imidazoline ring would improve corrosion inhibition efficiency of imidazoline derivatives [6]. According to studies of the drag reducing effect of inhibitors using a microelectrode array incorporated flus into a surface impinged with a submerged jet, it has been reported that inhibitors reduced the wall shear stress dependent on their chemical structure and concentration [7]. On the other hand, it was suggested that the inhibitors increase the Young's modulus of the corrosion product scale because inhibitors molecule replaced water molecule in the pore of the corrosion scale, so the inhibitors strengthened the corrosion scale, enhancing the protectiveness of this corrosion scale [8].

It has been reported that the efficiency of inhibitors may be influenced by the presence of the oily phase. It seems that the presence of the oily phase has an effect of coadsorption of the inhibitor on the substrate to improve the inhibitor performance. This behavior has been observed mainly in oil-soluble inhibitors, and it is affected by the different solubilities and the hydrophobic characters of the inhibitors in the two environments (water-oil) [2]. However, in absence of the oily phase, the inhibitor performance may be compromised and it is therefore important to determine how the inhibitor works in absence of the oily part.

The corrosion rate of carbon steels in neutral NaCl solutions is initiated through two main mechanisms: formation and build-up of an iron oxide layer and partial destruction of this layer by pitting [9]. In these conditions, it is recognized that the oxygen reduction reaction (ORR) plays a key role on the corrosion process in the solutions containing sodium chloride, which is an important composition in seawater and some industry environments. The ORR is influenced by the type of material, pretreatment, passive film developed,  $\text{Cl}^-$  concentration, pH and inhibitor used [9-14].

The goal of this work is to study the effectiveness and electrochemical behavior of two imidazole-based inhibitors on the corrosion behavior of the carbon steel in 3% NaCl solution by using standard electrochemical techniques as polarization curves, electrochemical impedance spectroscopy (EIS), and linear polarization resistance (LPR) measurements.

## 2. EXPERIMENTAL PROCEDURE

### 2.1. Material

The chemical composition (wt.%) of 1018 carbon steel used was 0.190 C, 0.670 Mn, 0.0003 P, 0.001 S, and balance Fe. Cylindrical specimens (4.55 cm length, 0.63 cm diameter) were polished with 600 grit silicon carbide emery paper and then cleaned with alcohol, acetone, and distilled water.

### 2.2. Testing solution

Two types of imidazolines, namely, hydroxyethyl (HEI-12), and hydroxyethyl modified with oleic chain from coconut oil (HEI-M), were used in this study. With a molecular structure as shown on Figure 1, this is composed of a five-member ring containing nitrogen elements, a pendant hydroxyethyl group attached to one of the nitrogen atoms and a hydrophobic head group. Hydrophobic head group was an alkyl chain of C12 for HEI-12, and an oleic chain from coconut oil for HEI-M. The inhibitors were dissolved in pure 2-propanol. The concentration of the inhibitor used in this work was 25 ppm for HEI-12 and 10 ppm for HEI-M. Testing solution consisted of 3% NaCl solution and the temperature kept at 50°C. Inhibitor was added 2 h after pre-corroding the specimens in the solution, starting the measurements 1 h later.

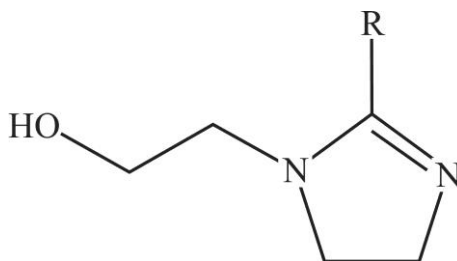


**Figure 1.** Molecular formulas of the hydroxyethyl imidazoline-type inhibitors used; where R alkyl chain of C12 for HEI-12, and oleic chain from coconut oil for HEI-M.

### 2.3. Electrochemical measurements

Employed electrochemical techniques included potentiodynamic polarization curves, linear polarization resistance, and electrochemical impedance spectroscopy measurements. Measurements were obtained by using a conventional three electrodes glass cell with graphite electrode as counter electrode and a saturated calomel electrode (SCE) as reference with a Lugging capillary bridge (Figure 2). Electrochemical techniques employed included potentiodynamic polarization curves, linear polarization resistance, and electrochemical impedance spectroscopy, measurements. Polarization curves were recorded at a constant sweep rate of 60 mV/min, and the scanning range was from -300 to +300 mV with respect to the open circuit potential,  $E_{corr}$ . The sweep rate of 1 mV/s is considered to guarantee obtaining steady-state current-potential curves [9]. Inhibition efficiencies [E(%)] were

determined from the corrosion current densities calculated by the Tafel extrapolation method according to the following equation:

$$E(\%) = \left[ \frac{i_b - i_i}{i_b} \right] * 100$$

where  $i_b$  is the corrosion rate without inhibitor and  $i_i$  the corrosion rate in the solution with inhibitor.

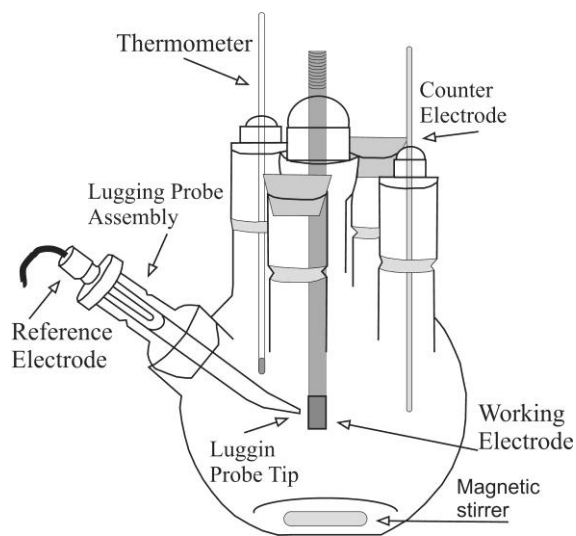


**Figure 2.** Scheme showing the experimental set-up for electrochemical measurements

Linear polarization resistance measurements were carried out by polarizing the specimen from +10 to -10 mV with respect to  $E_{corr}$ , at a scanning rate of 1 mV/s. Electrochemical impedance spectroscopy tests were carried out at  $E_{corr}$  by using a signal with amplitude of 10 mV and a frequency interval of 0.01–100 kHz. An ACM potentiostat controlled by a desk top computer was used for the LPR tests and polarization curves, whereas for the EIS measurements, a model PC4 300 Gamry potentiostat was used. All the tests were carried out at 50 °C and lasted for 24 h and started 30 min after addition of the inhibitor, taking readings every hour.

### 3. RESULTS AND DISCUSSION

#### 3.1. Polarization curves

Figure 3 shows the polarization curves for 1018 carbon steel in 3% NaCl solutions in absence and presence of inhibitors. In the absence of inhibitor there was only an active behavior, without the formation of a passive layer showing that the formation of corrosion products layer was not protective. The  $I_{corr}$  value was calculated from the cathodic branch of polarization curve as shown in Figure 4, in agreement as other authors have suggested for non-Tafel dependence curves [2-5].

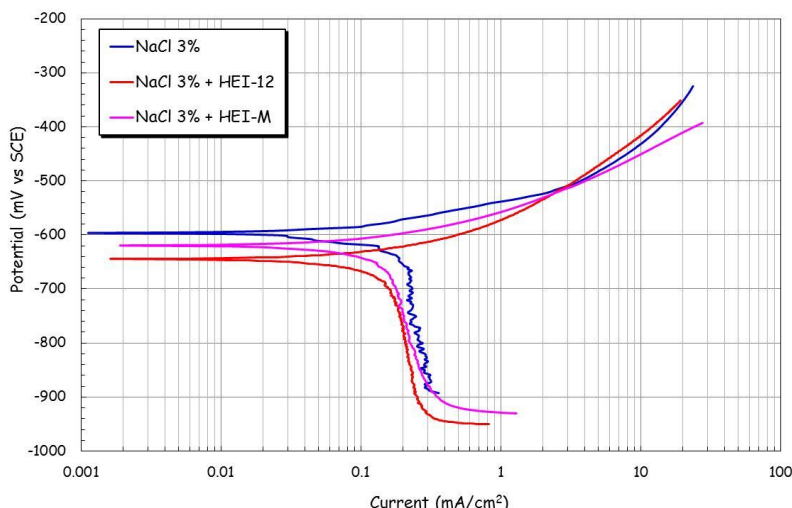


**Figure 3.** Effect of HEI-12 and HEI-M in the polarization curves for 1018 carbon steel in 3% NaCl solution at 50°C.

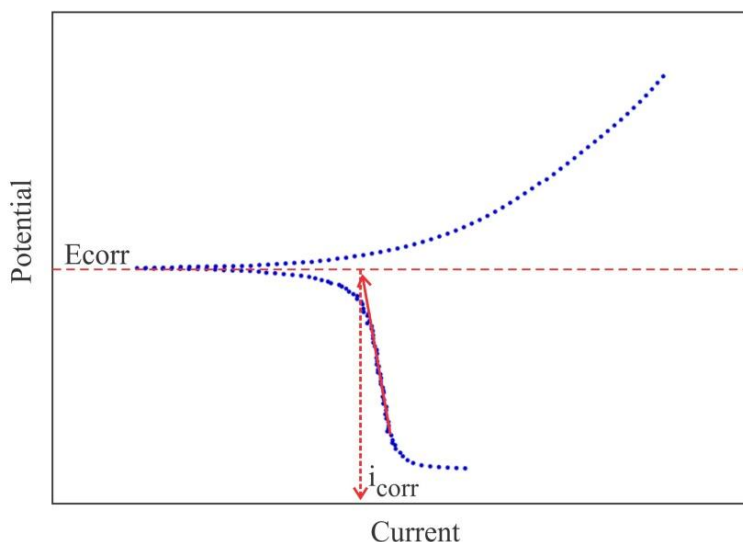


**Figure 4.** Calculation of  $I_{corr}$  for non-Tafel dependence curves.

As the inhibitor was added, the  $E_{corr}$  value was shifted towards more active values and the  $I_{corr}$  values was slightly reduced. Anodic branches show an active behavior, similar to that observed for the solution without inhibitor. This behavior may be due that none of the inhibitors is water-soluble, and the inhibitor solubility only is favored by the temperature in order to they are more easily transported towards the surface to be adsorbed to form a film against corrosion. On the cathodic branch, a cathodic limiting current can be seen, which is due to the oxygen reduction. It can see that no significant effect of the inhibitors was found on the cathodic branch of the polarization curve, since the limiting current density remained almost unaltered with the presence of HEI-12 and HEI-M inhibitors. It also notes that the cathodic branches slope does not vary significantly, it has been reported that the cathodic Tafel slope is independent of the dissolved oxygen concentration [15].

It has been reported that in absence of oxygen, the primary cathodic reactions are dependent on the pH solution. At a low pH value, H<sup>+</sup> reduction is the dominant cathodic reaction because of the high H<sup>+</sup> concentration [5]. In this condition, there is an increase in corrosion rate due to increase in acidity. This behavior results from sufficient supply of hydrogen ion leading to hydrogen reduction reaction as well as presence of chloride ions which lead to pitting [11-12]. However, in not deaerated systems the dominant cathodic reaction is the oxygen reduction reaction, where this one is a multielectron reaction that may include a number of elementary steps involving different reaction intermediates [16]. It has been proposed that the possible reduction reactions are:

- Addition of the first electron to the oxygen dissolved:



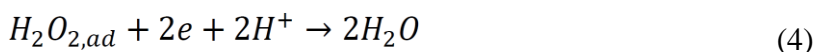
- Directly to water:



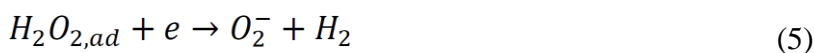
- Reduced to H<sub>2</sub>O<sub>2,ad</sub>:



- The adsorbed peroxide can be electrochemically reduced to water:



- Decomposed on the electrode surface:



- Or desorbed into the bulk of the solution:



In either case, the rate determining step appears to be the addition of the first electron to the oxygen dissolved (equation 1) [16]. Different studies [10, 13, 16] suggest that a pathway via an (H<sub>2</sub>O<sub>2</sub>)<sub>ad</sub> intermediate may be the operative pathway for the reduction of the dissolved oxygen. Where dissolved oxygen is reduced to H<sub>2</sub>O (equation 4), via equation 1 and 3.

It has been reported that a decrease in the cathodic current corresponds to a decrease in the limiting current density for oxygen reduction on the carbon steel surface, which is a result of increasing resistance to oxygen diffusion exerted by oxide layer build-up [9]. In our case, the limit current observed is two orders of magnitude smaller since the availability of dissolved oxygen depends

on the test temperature. This is a consequence that the amount of oxygen that can be held by the water depends on the water temperature, salinity, and pressure. Gas solubility decreases with increasing temperature, increasing salinity, or decreasing pressure.

Table I summarizes the electrochemical parameters obtained for the polarization curves. From this table and the polarization curves shown in Figure 3 it can be said that both inhibitors behave as anodic inhibitors and the HEI-M had the best performance. However, it should be noted that this behavior correspond to the beginning of the corrosion process, and this trend may change in long-term exposures.

**Table 1.** Electrochemical parameters for 1018 carbon steel in 3% NaCl and the different types of imidazolines

Inhibitor	$E_{corr}$ (mV)	$I_{corr}$ (mA cm <sup>-2</sup> )	$b_a$ (mV/decade)	$b_c$ (mV/decade)	$E$ (%)
Blank	596	0.19	69	1292	---
HEI-12	645	0.15	85	1226	21
HEI-M	619	0.14	73	845	26

### 3.2. Free Corrosion Potential Curves

$E_{corr}$  as a function of time is presented in Figure 5. It is known that a simple way to study the film formation and passivation of materials in a solution is to monitor the  $E_{corr}$  as a function of time. A rise of potential in the positive direction indicates the formation of a passive film, a steady potential indicates that the film remains intact and protective, and a drop of potential in the negative direction indicates breaks in the film, dissolution of the film, or no film formation [17].

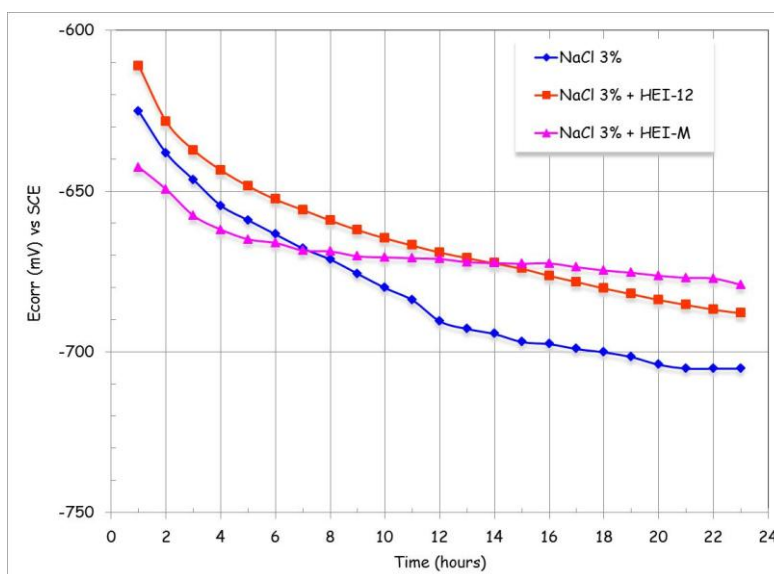


**Figure 5.** Effect of HEI-12 and HEI-M in  $E_{corr}$  values for 1018 carbon steel in 3% NaCl solution at 50°C.

It can be seen that 1018 carbon steel behavior either with and without inhibitor addition has the same trend, i.e., the corrosion potential values decrease with time. Then, the inhibitory power of the imidazoline-based compounds observed in polarization tests is affected when this one is evaluated over time. However,  $E_{corr}$  values with inhibitor addition are slightly higher than those observed without inhibitor addition. The  $E_{corr}$  values decreasing rate of HEI-M inhibitor is lower than that observed with HEI-12 inhibitor. However, both values show tendency to coincide with those values without inhibitor addition. These results show that in all cases, 1018 carbon steel experience an active corrosion process due to the poor stability of the developed protective layer and the poor coverage of the inhibitors, which are not efficiently protecting it.

### 3.3. LPR curves

The variation in the  $I_{corr}$  values for the 3% NaCl solution with and without the addition of the inhibitors are given in Figure 6. It is known that once polarization resistance is determined, calculation of  $I_{corr}$  requires knowledge of the Tafel constants, and these constants can be determined from experimental polarization curves. Also, in the absence of these values, an approximation is sometimes used, and the expected error in the calculated value of  $I_{corr}$  should be less than a factor of two [18]. However, when the results show polarization resistance values within the same order of magnitude, it is necessary to use more precise values of the Tafel slopes in order to perform a reliable analysis of the results [19]. Therefore, the values shown in Figure 6 were obtained from the polarization resistance measurements using Stern-Geary expression [18].

$$I_{corr} = \frac{b_a b_c}{2.3R_p(b_a + b_c)} = \frac{B}{R_p}$$

where the  $b_a$  and  $b_c$  values were those reported in Table 1.

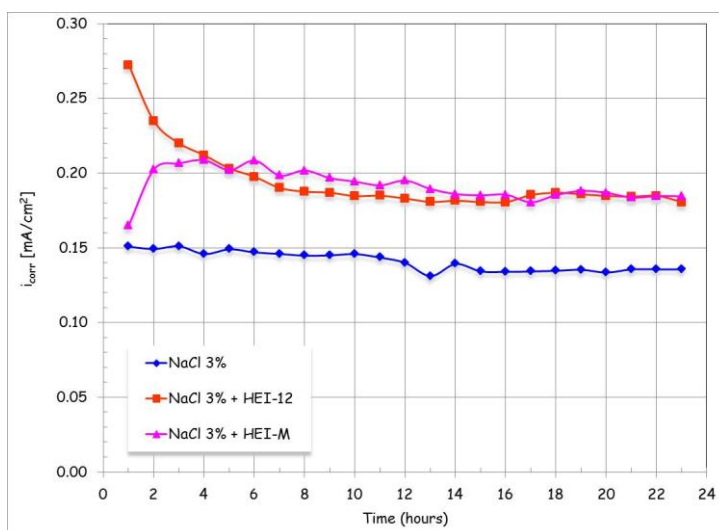
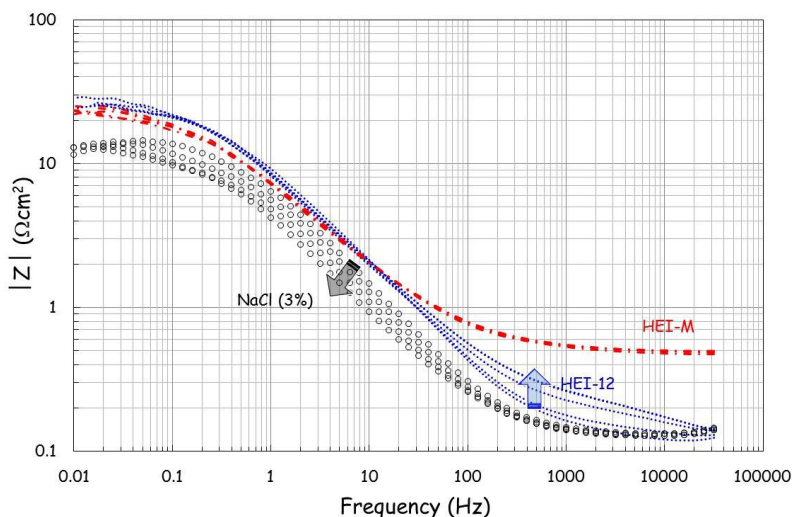


**Figure 6.** Effect of HEI-12 and HEI-M on the change in the  $I_{corr}$  value with time for 1018 carbon steel in 3% NaCl solution at 50°C.

The polarization resistance tests shown that 1018 carbon steel behavior either with or without inhibitor addition had the same trend, i.e., the  $I_{corr}$  values show a tendency to decrease slightly over time. However,  $I_{corr}$  values with inhibitor addition are slightly higher than those observed without inhibitor addition. In particular, those solutions with the presence of inhibitor tend to converge to the same values. This indicates that for long periods of exposure inhibitors show the same efficiency, and notwithstanding that the corrosion rates are slightly higher than those observed in the solution without inhibitor, such are within the same order of magnitude. The low efficiency of protection of inhibitors is mainly due to its low solubility in the aqueous medium, which limits its diffusion to the metal surface. It has been reported that the presence of an oily phase, such as diesel, improves the efficiency of the inhibitors because its solubility in the aqueous phase is increased and they can be more easily transported towards the metal surface [2, 5].

### 3.4. EIS results

Figure 7 discloses the Bode diagrams of the 1018 carbon steel in 3% NaCl solution in absence and presence of inhibitors. It is said that the impedance spectrum can be considered as a “finger print”, which is related to the transient behavior of a specific electrochemical interface, and it reflects dielectric behavior, oxidation–reduction reactions and mass migration across the electrochemical interface, which are determined by the electrical and chemical properties of the corrosive medium, and the electrode materials [14]. Also, analysis of the Bode diagram is simpler than the Nyquist diagrams. Bode format minimizes the dispersion of the experimental data and shows a clearer description of the frequency-dependent behavior of the electrochemical system, which only is implicit in the Nyquist diagrams. In addition, Bode diagrams are most appropriate for analysis and extrapolation of the experimental data at low frequencies. From the Bode diagram can also be identified the following basic elements in order to establish the configuration of the equivalent circuits describing the electrochemical system [20]; resistors ( $R$ ) that appear as plateaus, and in this case  $|Z| = R$  and  $\phi \rightarrow 0^\circ$ , capacitors ( $C$ ), where  $|Z|$  is a straight line with a  $-1$  slope and  $\phi \rightarrow 90^\circ$ , elements associated with *diffusion*, where  $|Z|$  has a  $-0.5$  slope and  $\phi = 45^\circ$ .



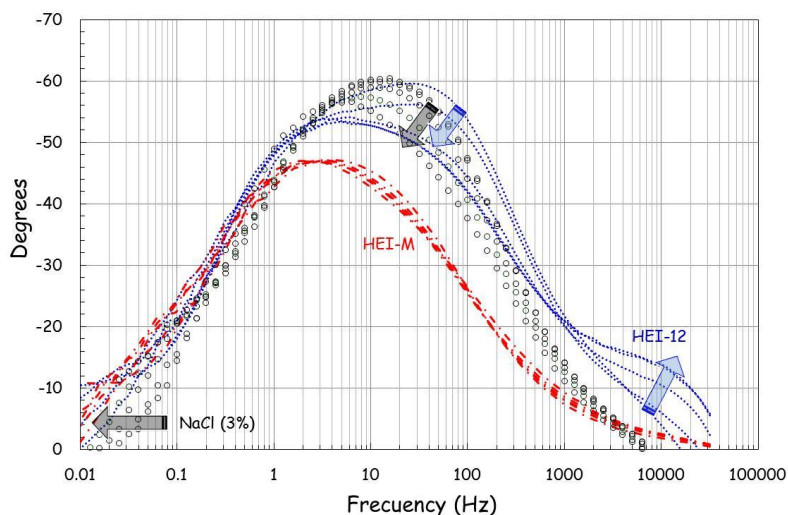


**Figure 6.** Effect of HEI-12 and HEI-M in the evolution of the Bode plots for 1018 carbon steel in 3% NaCl solution at 50°C.

In general, three frequency regions referring to the high, intermediate and low frequency values are obtained from Bode diagrams [21-22]. In the higher frequency region ( $f > 1000$  Hz), the Bode plot exhibits a plateau (horizontal line) of the  $|Z|$  values with the phase angle approaching  $0^\circ$ . This is the response of the electrode ohmic or solution resistance,  $R_s$ , which includes the electrolyte resistance, cell geometry, impedance of the conductors and the reference electrode. In the middle frequency region (1000 to 10 Hz), the spectrum display the maximum phase angle approaching  $-90^\circ$  and a linear slope of about -1 in  $\log |Z|$  as  $\log (f)$  decreases. This is the characteristic response of capacitive behavior of the electrode and describes the dielectric properties of the electronically conducting surface film. In the lower frequency region ( $f < 10$  Hz) its detected the electron charge transfer process, the mass transfer processes, or other relaxation processes taking place at the film–electrolyte interface or within the pores of the surface film.

In all cases from Bode diagram (Figure 6) is observed that in the high frequency range ( $>1000$  Hz), the  $\log |Z|$  values tend to a constant ( $\log |Z|$  becomes independent of frequency) where the phase angle approaches zero. This behavior is consistent in the uninhibited solution and in the solution inhibited with HEI-M. In the solution with HEI-12 inhibitor, the plateau region begins to form at frequencies above 30 kHz, and the formation of a new phase angle loop is also observed. According to other authors [3], this new loop can be ascribed to the inhibitor film because its small time constant causes a phase shift in the high frequency region, since the presence of a long hydrocarbon chain in the structure of the imidazoline is responsible for their capacity of forming protective barriers against aggressive ions from the bulk solution. On the other hand, in the case of the inhibited solution with HIE-M was not observed the formation of a new loop, and on the contrary it was observed an increase in the solution resistance. It is possible that in this case, due to the low solubility of the inhibitor the solution became more resistive.

In the intermediate frequency region ( $1.0 < f < 1000$  Hz, in this study), in all cases there is a linear relationship between  $\log |Z|$  and  $\log f$ . The values of slopes are lower than -1, and phase angles

values less than  $90^\circ$ . These two facts indicate that the developed oxide layer has no capacitive nature, and that the corrosion process can be under mixed control (diffusion and charge transfer). In the case in the uninhibited solution and solution with HEI-12, it is observed the presence of a single phase shift between 20-30 Hz, which is shifting to lower frequencies as time elapses. In addition, this change is associated with a decrease of the phase angle. The uninhibited solution shows a steady decrease in the slope of the  $\log |Z|$ - $\log f$  relation, and this does not occur in inhibited solutions where this one remains constant. This may be due to the development of a porous oxide layer with non-protective characteristics, and the corrosion process becomes controlled by the diffusion of the corrosive specie. In the inhibited solution with HEI-M no appreciable changes are observed in the spectrum as time elapses, in this case the slope of the  $\log |Z|$ - $\log f$  relation has the smallest value (close to 0.5), and the phase angle remains unchanged (close to  $-45^\circ$ ) at 2-3 Hz frequency value. Therefore, it can be established that in the case of the inhibited solution with HEI-M, the corrosion process is mainly controlled by diffusion of the aggressive ions, as it has been noted that a diffusion process is associated with a  $\log |Z|$ - $\log f$  slope value of 0.5 and a phase angle value of  $45^\circ$  [20].

In the low frequency region ( $f < 1.0$  Hz, in this study), in all cases it is observed that the  $\log |Z|$  values tend to a constant (impedance is independent of the frequency) and the phase angle approximates to zero. The maximum values observed in the plateau region show a tendency to decrease over time which confirms an active corrosion process. These values are greater than those of the uninhibited solution and their values tend to the same value, this is consistent with the results observed in measurements of LPR (Figure 6). In the case of the uninhibited solution, it is observed a shift toward smaller frequencies of the phase angle, and this one trends to zero at frequencies below 0.01 Hz. Also, a scattering in the experimental data is observed in this region. This behavior is associated with a contraction of  $Z_{\text{real}}$  as it could be observed in the Nyquist plot. Some authors suggest that in 3.5% NaCl solutions, the oxygen reduction reaction is a mass-transfer controlled 4-electron process [13] and it can show three different diffusion characters [10], where the first one happens when the thickness of stagnant layer is infinite and it is called semi-infinite diffusion process (Warburg diffusion), the second one it is a transmissive finite diffusion process with real part contraction and it happens when the thickness of the stagnant layer is finite, and the third one is a reflective finite diffusion process, which happens when only the transmission takes place in a limited distance. Therefore, it can be considered that in all cases (uninhibited and inhibited solutions) there is a transmissive finite diffusion process. Where in the uninhibited solution it was due to the porous oxide layer developed, and in the inhibited solution with HEI-12 it was due to inhibitor film formation where the presence of long hydrocarbon chains in the structure of the imidazolines is responsible for their capacity of forming protective barriers against aggressive ions from the bulk solution [3]. In the inhibited solution with HEI-M, an increase in the solution resistivity limited the diffusion of the aggressive ions as it was evidenced in their impedance spectrum, since they did not vary significantly depending on the time. In addition, it was evident that there was no evidence of the formation of a protective film because there was only one capacitive loop in the EIS Nyquist plots.

#### 4. CONCLUSIONS

A study on the effect of two imidazoline-based inhibitors in NaCl 3% solutions on the corrosion performance of 1018 carbon steel by using different electrochemical techniques was carried out. The different electrochemical techniques showed that there was not a significant improvement by the addition of additives on the corrosion resistance of the substrate. The poor performance of the inhibitors was due to its low solubility in the aqueous phase. According to the EIS studies, it was observed that the HEI-12 inhibitor was capable of being adsorbed onto the substrate surface but was unable to form a continuous protective film to prevent the corrosion of the substrate. In the case of HEI-M inhibitor was not observed the formation of an inhibitor film onto the substrate surface. The HEI-M inhibitor increased the resistivity of the solution and thereby limited the aggressive ions diffusion at the substrate surface. In all cases there was an active corrosion process where diffusion became rate-determining step of the corrosion process as time passes.

#### ACKNOWLEDGMENTS

Financial support from Consejo Nacional de Ciencia y Tecnología (CONACYT, México) (Project 83164 and Ph.D. scholarship to L.M. Rivera-Grau) is gratefully acknowledged. Authors are also grateful to DGAPA-UNAM for Ignacio Regla's sabbatical fellowship at ICF-UNAM and financial support from CONACYT through Proinnova Projects 155331 and 155342.

#### References

1. P.C. Okafor, X. Liu and Y.G. Zheng, *Corros. Sci.*, 51 (2009) 761.
2. W. Villamizar, M. Casales, J. G. Gonzalez-Rodriguez and L. Martinez, *J Solid State Electrochem*, 11 (2007) 619.
3. W. Villamizar, M. Casales, L. Martinez, J. G. Chacon-Naca and J. G. Gonzalez-Rodriguez, *J Solid State Electrochem*, 12 (2008) 193.
4. D.M. Ortega-Toledo, J.G. Gonzalez-Rodriguez, M. Casales, M.A. Neri-Flores and A. Martinez-Villafañe, *Mater. Chem. Phys.*, 122 (2010) 485.
5. D. M. Ortega-Sotelo, J. G. Gonzalez-Rodriguez, M. A. Neri-Flores, M. Casales, L. Martinez and A. Martinez-Villafañe, *J Solid State Electrochem*, 15 (2011) 1997.
6. Daxi Wang, Shuyuan Li, Yu Ying, Mingjun Wang, Heming Xiao and Zhaoxu Chen, *Corros. Sci.*, 41 (1999) 1911.
7. G. Schmitt, C. Bosch, H. Bauer and M. Mueller, *Proceeding of NACE Corrosion/2000*, Paper No. 2.
8. S. Ramachandran, S. Campbell and M.B. Ward, *Proceeding of NACE Corrosion/2000*, Paper No. 25.
9. Luis Cáceres, Tomás Vargas and Leandro Herrera, *Corros. Sci.*, 51 (2009) 971.
10. Fei Kuang, Dun Zhang, Yongjuan Li, Yi Wan and Baorong Hou, *J Solid State Electrochem*, 13 (2009) 385.
11. H.T. Kim, C.H. Paik, W.I. Cho, B.W. Cho, K.S. Yun, Y.H. Kim, J.B. Ju, J.S. Kim, M.S. Kang, J.S. Ha and K.Y. Kim, *Journal of Ind. & Eng. Chemistry*, 3 (1997) 51.
12. K. Jafarzadeh, T. Shahrabi, S.M.M. Hadavi and M.G. Hosseini, *J. Mater. Sci. Technol.*, 23 (2007) 623.
13. Li Yongjuan, Zhang Dun, and Wu Jiajia, *J. Ocean Univ. China*, 9 (2010) 239.
14. C. Liu, Q. Bi, A. Leyland and A. Matthews, *Corros. Sci.*, 45 (2003) 1243.

15. S. Hiromoto, A.-P. Tsai, M. Sumita and T. Hanawa, *Corros. Sci.*, 42 (2000) 2167.
16. N. M. Markovic, T. J. Schmidt, V. Stamenkovic and P. N. Ross, *Fuel Cells*, 1 (2001) 105.
17. I. Gurappa, *Materials Characterization*, 49 (2002) 73.
18. E.E. Stansbury and R.A. Buchanan, *Fundamentals of Electrochemical Corrosion*, ASM International, Ohio (2000).
19. A. Pardo, S. Feliu Jr., M. C. Merino, R. Arrabal, and E. Matykina, *International Journal of Corrosion*, 2010 (2010) Article ID 953850.
20. Viatcheslav Freger and Sarit Bason, *J. Membrane Sci.*, 302 (2007) 1.
21. J.E.G. Gonzalez and J.C. Mirza-Rosca, *J. Electroanal. Chem.*, 471 (1999) 109.
22. S. Tamilselvi, V. Raman and N. Rajendran, *Electrochim. Acta*, 52 (2006) 839.